PROCEEDINGS OF SCIENCE

# Proton lifetime bounds from chirally symmetric lattice QCD

**RBC and UKQCD Collaborations**

**Paul Cooney***
*University of Edinburgh, UK*
*E-mail:* p.cooney@sms.ed.ac.uk

We present results for the matrix elements relevant for proton decay in Grand Unified Theories (GUTs). The calculation is performed at a fixed lattice spacing $a^{-1} = 1.73(3)$ GeV using 2+1 flavors of domain wall fermions on lattices of size $16^3 \times 32$ and $24^3 \times 64$ with a fifth dimension of length 16. We use the indirect method which relies on an effective field theory description of proton decay, and we estimate the low energy constants, $\alpha = -0.0112(25)$ GeV$^3$ and $\beta = 0.0120(26)$ GeV$^3$. We relate these low energy constants to the proton decay matrix elements using leading order chiral perturbation theory.

*The XXVI International Symposium on Lattice Field Theory*
*July 14 - 19, 2008*
*Williamsburg, Virginia, USA*

*Speaker.

 

PoS(LATTICE 2008)283

## 1. Introduction

Proton decay is a distinctive signature of many Grand Unified Theories (GUTs) although it has yet to be observed experimentally. This non-observation of proton decay has already ruled out the simplest minimal supersymmetric models [1]. The current minimum bound on the proton lifetime from Super–Kamiokande is $8.2 \times 10^{33}$ years [2].

One expected decay channel for a proton $N$ is $N \to M + l$, with $M$ a pseudoscalar meson and $l$ a lepton. This decay is induced by the exchange of either heavy gauge bosons or supersymmetric particles. By integrating out these heavy particles, we obtain an effective Lagrangian which describes the low–energy behaviour. The partial decay width is proportional to the hadronic matrix element $\langle M|\mathscr{O}|N\rangle$ with $\mathscr{O}$ the operator from the effective Lagrangian. A quantitative estimate of the matrix element is desired to probe the GUT scale physics of our models at current experiments.

There have been many previous attempts to measure the matrix elements [3, 4, 5, 6, 7, 8, 9, 10, 11, 12, 13, 14, 15, 17]. In this proceedings we present a determination of the matrix elements using dynamical Domain Wall Fermion (DWF) configurations with $2+1$ flavours. Our results have been published in [16] and extend the ones obtained for 2 flavours of dynamical DWF in Ref. [17].

## 2. Partial proton decay width

For a generic proton decay channel, the partial decay width is,

$$\Gamma(N \to M + \bar{l}) = \left[\frac{m_N}{32\pi^2}\left(1 - \left(\frac{m_M}{m_N}\right)^2\right)^2\right]\left|\sum_i C^i W_0^i(N \to M + \bar{l})\right|^2 \tag{2.1}$$

where $m_N$ is the mass of the proton and $m_m$ the mass of the meson. $C^i$ are the Wilson coefficients from the effective Lagrangian and the form factors $W_0$ can be related to the hadronic matrix elements

$$P_L\left[W_0^i(q^2) - i\not{q}W_q^i(q^2)\right]u(k,s) = \langle M|\mathscr{O}^i|N\rangle \tag{2.2}$$

The three quark operators $\mathscr{O}^i$ that apear in the partial width were identified on symmetry grounds in Refs. [18, 19, 20] and are given by

$$\mathscr{O}^{RL} = \varepsilon^{abc}u^{a,T}(x,t)CP_R d^b(x,t)P_L u^c(x,t) \tag{2.3}$$

$$\mathscr{O}^{LL} = \varepsilon^{abc}u^{a,T}(x,t)CP_L d^b(x,t)P_L u^c(x,t) \tag{2.4}$$

Operators of this form will be used throughout this paper, so we choose to define a generic three quark operator

$$\mathscr{O}^{\Gamma_i\Gamma_j} = \varepsilon^{abc}u^{a,T}(x,t)C\Gamma_i d^b(x,t)\Gamma_j u^c(x,t) \tag{2.5}$$

where $\Gamma_i$ are matrices with two spin indices, labelled by $S = 1$, $P = \gamma_5$, $V = \gamma_\mu$, $A_\mu = \gamma_\mu\gamma_5$, $T = \frac{1}{2}\{\gamma_\mu, \gamma_\nu\}$, $\tilde{T} = \gamma_5\frac{1}{2}\{\gamma_\mu, \gamma_\nu\}$, $R = P_R = \frac{1}{2}(1+\gamma_5)$ and $L = P_L = \frac{1}{2}(1-\gamma_5)$

Using chiral perturbation theory to compute the matrix element in Eq. (2.2) yields for the $N \to \pi$ transition [14, 21]:

$$\langle\pi^0|\mathscr{O}^{RL}|N(\mathbf{k},s)\rangle \simeq \alpha P_L u(\mathbf{k},s)\left[\frac{1}{\sqrt{2}f} + \frac{D+F}{\sqrt{2}f}\right] + O(m_l^2/m_N^2), \tag{2.6}$$

$$\langle\pi^0|\mathscr{O}^{LL}|N(\mathbf{k},s)\rangle \simeq \beta P_L u(\mathbf{k},s)\left[\frac{1}{\sqrt{2}f} + \frac{D+F}{\sqrt{2}f}\right] + O(m_l^2/m_N^2), \tag{2.7}$$

where $\alpha$ and $\beta$ are two low–energy constants (LECs) from the proton decay Lagrangian, $m_l$ is the mass of the lepton and $f$ is the pion decay constant. The combination $F+D$ yields the nucleon axial charge, $g_A = 1.2695(29)$ [22], while the combination $F-D$ is related to the ratio of the zero–momentum form factors for semileptonic hyperon decay, $g_1/f_1$ [23]. The LECs can be calculated at leading order from the proton to vacuum matrix elements.

$$\langle 0|\mathscr{O}^{RL}|N(\mathbf{k},s)\rangle = \alpha P_L u(\mathbf{k},s) \quad \langle 0|\mathscr{O}^{LL}|N(\mathbf{k},s)\rangle = \beta P_L u(\mathbf{k},s), \tag{2.8}$$

These same LECs appear in the expressions for other matrix elements (eg. $N \to K^+$), see Ref [24].

## 3. Results

The analysis was performed on 2+1 flavor DWF ensembles with two different volumes at a fixed inverse lattice spacing of $a^{-1} = 1.73(3)$ GeV. These are described fully in Refs. [25] and [26]. Multiple sources per configuration and several different types of smearing have been used to improve the signal. As well as local sources ($L$), we employ gauge–invariant Gaussian smearing with two different smearing radii ($G$ and $G*$) and gauge fixed hydrogen–like wavefunction smearing ($H$). We adopt the same convention used in Ref. [27] for naming the smeared two–point functions.

We now define a class of two–point correlation functions

$$f_{\Gamma_1\Gamma_2,\Gamma_3\Gamma_4}(t) = \sum_x \mathrm{tr}\left[\langle \mathscr{O}^{\Gamma_1\Gamma_2}\bar{\mathscr{O}}^{\Gamma_3\Gamma_4}\left(\frac{1+\gamma_4}{2}\right)\right] \tag{3.1}$$

with $P = \frac{1}{2}(1+\gamma_4)$ a projection matrix, and $\mathscr{O}^{\Gamma_i\Gamma_j}$ as defined in Eq 2.5. For example, $f_{PS,PS}$ is the usual proton correlation function.

We can obtain the LECs from the vacuum matrix elements in Eq. 2.8 by forming ratios of two–point functions.

$$R_\alpha(t) = 2G_N \frac{f_{RL,PS}(t)}{f_{PS,PS}(t)} \to \alpha \quad R_\beta(t) = 2G_N \frac{f_{LL,PS}(t)}{f_{PS,PS}(t)} \to \beta \tag{3.2}$$

where $G_N$ is the proton amplitude defined from the overlap of the proton interpolating field, to the normalized proton state.

$$\langle 0|\mathscr{O}^{PS}(\vec{0},0)|N(\mathbf{k},s)\rangle = G_N u(\mathbf{k},s). \tag{3.3}$$

Therefore, in order to calculate the LECs, first we calculate the proton mass $m_N$ from a correlated fit to the effective mass of the proton correlation function $f_{PS,PS}$,

$$m_{N,\mathrm{eff}}(t) = \log\left[\frac{f(t)}{f(t+1)}\right] \tag{3.4}$$

In all our correlated fits, we used an unfrozen correlation matrix. See Ref. [28] for analysis of different estimates of the correlation matrix.

Second we calculate the proton amplitude from a correlated fit to an effective amplitude

$$G^2_{N,\mathrm{eff}}(t) = \frac{1}{2} f_{PS,PS}(t)\exp(m_N t), \tag{3.5}$$

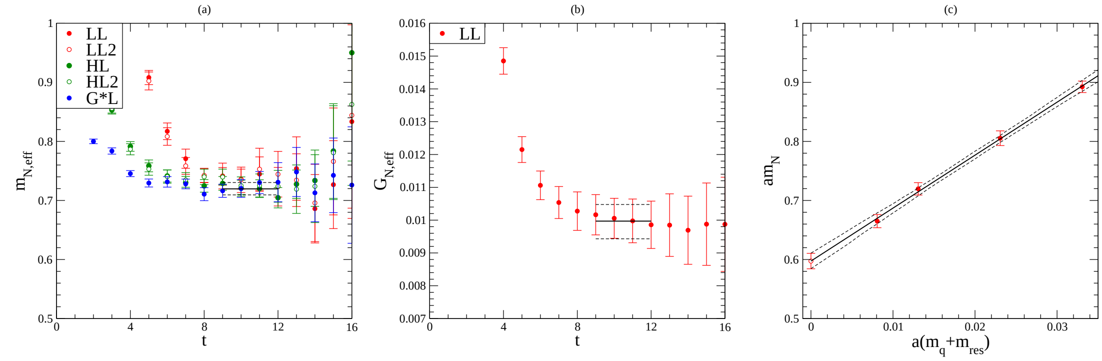


**Figure 1:** (a) is an effective mass plot and (b) is an effective amplitude plot for the nucleon. Both are calculated on the $24^3 \times 64$ dataset with $am_u = 0.01$. The different colours in the effective mass plot correspond to different smearings. Datasets are labelled with the smearing, i.e. LL. Those datasets labelled with a 2 use the operator $f_{A_4S,A_4S}(t)$, the rest use $f_{PS,PS}(t)$. ( c ) is a linear extrapolation of the ground state mass to the chiral limit.

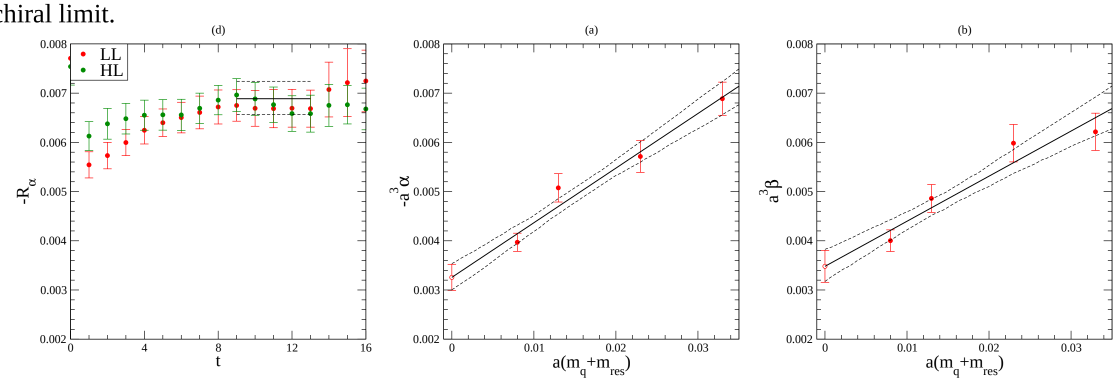


**Figure 2:** (a) shows the ratio $R_\alpha$ in Eq. 3.2 for the $24^3 \times 64$ dataset with $am_u = 0.03$. The different colours correspond to different source smearing. Horizontal lines show the fit to the plateau. Also shown are linear chiral extrapolation for the ratios $R_\alpha$ (b) and $R_\beta$ (c) for the $24^3 \times 64$ dataset.

which uses the value of the proton mass we just calculated. Examples of an effective mass plot and an effective amplitude plot are given in Fig. 1. along with a plot of an extrapolation of the nucleon mass to the chiral limit.

Finally we calculate the LECs from the ratio in Eq. 3.2. An example plot for $\alpha$ is given in Fig. 2 along with extrapolations to the chiral limit for both $\alpha$ and $\beta$. Results from each of these fits as well as results for the nucleon mass are summarised in Table 1.

## 4. Non–perturbative renormalization

For the non–perturbative renormalization (NPR) we use the MOM scheme renormalization of the Rome-Southampton group. The renormalised operators are

$$\mathcal{O}^A_{\rm ren} = Z^{AB}\mathcal{O}^B_{\rm latt} \tag{4.1}$$

| $V \times L_s$ | $am_{ud}/am_s$ | $am_N$ | $a^3\alpha$ | $a^3\beta$ |
|---|---|---|---|---|
| | 0.03/0.04 | 0.908(6) | -0.00695(19) | 0.00719(21) |
| $16^3 \times 32 \times 16$ | 0.02/0.04 | 0.819(8) | -0.00605(31) | 0.00606(30) |
| | 0.01/0.04 | 0.722(19) | -0.00478(43) | 0.00511(47) |
| | chiral | | -0.00349(64) | 0.00369(63) |
| | 0.03/0.04 | 0.892(10) | -0.00689(33) | 0.00621(38) |
| $24^3 \times 64 \times 16$ | 0.02/0.04 | 0.805(12) | -0.00571(32) | 0.00598(38) |
| | 0.01/0.04 | 0.720(10) | -0.00508(29) | 0.00486(28) |
| | 0.005/0.04 | 0.671(5) | -0.00397(18) | 0.00400(22) |
| | chiral | | -0.00326(27) | 0.00348(32) |

**Table 1:** Results from fits described in this paper. The nucleon masses the LECs $\alpha$ and $\beta$ are reported as a function of the quark masses, for both lattices used in this study. The results of linear chiral extrapolations are also reported in the last line of each column. All the results are given in units of the lattice spacing $a \approx 0.12$ fm.



where A and B label the spin structure from the nucleon decay operators, eg LL, RL. These mix with a third operator $\mathscr{O}^{A(LV)}$, so $Z^{AB}$ is a $3\times 3$ matrix. We shall call $\mathscr{O}^{LL}\mathscr{O}^{RL}$ and $\mathscr{O}^{A(LV)}$ the chirality basis of operators.

We want to calculate the non-perturbative amputated 3-quark vertex function of these operators

$$\mathscr{G}^{A}_{abc,\alpha\beta\gamma\delta}(p^2) = \varepsilon^{abc}(C\Gamma)_{\alpha'\beta'}\Gamma'_{\delta\gamma'}\langle Q^{a'a}_{\alpha'\alpha}(p)Q^{b'b}_{\beta'\beta}(p)Q^{c'c}_{\gamma'\gamma}(p)\rangle \tag{4.2}$$

where

$$Q^{a'a}_{\alpha'\alpha} = \langle S^{a'a''}_{\alpha'\alpha''}(p)\rangle^{-1} S^{a''a}_{\alpha''\alpha}(p) \tag{4.3}$$

and $\Gamma$ and $\Gamma'$ are the matrices which appear in $\mathscr{O}^{A}$

For convenience, we will work in the parity basis of operators SS-SP, PP-PS, AA+AV which are related to the chirality basis of operators we are interested in via

$$\begin{aligned} LL &= \frac{1}{4}(SS+PP) - \frac{1}{4}(SP+PS) \\ RL &= \frac{1}{4}(SS-PP) - \frac{1}{4}(SP-PS) \\ A(LV) &= \frac{1}{2}AA - \frac{1}{2}(-AV) \end{aligned} \tag{4.4}$$

We relate the amputated 3-quark vertex functions to the renormalization matrix Z by the renormalization condition. In the RI–Mom Scheme this is

$$Z_q^{-3/2} Z^{BC} M^{CA} = \delta^{BA} \tag{4.5}$$

Where the matrix $M$ is,

$$M^{AB} = \mathscr{G}^{A}_{abc,\alpha\beta\gamma\delta}(p^2) P^{B}_{abc,\beta\alpha\delta\gamma} \tag{4.6}$$

and the projection matrices $P^{A}_{abc,\beta\alpha\delta\gamma}$ are chosen so that the renormalization condition is satisfied in the free field case where $Z_q = 1$ and $Z^{BC} = \delta^{BC}$. An example of a plot of the matrix M, after

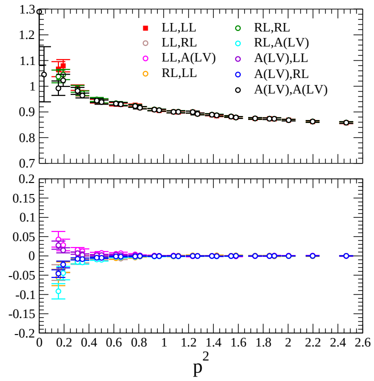


**Figure 3:** The mixing matrix $M$ in Eq. (4.6) in the chirality basis, $\Gamma\Gamma' = \{LL, RL, A(LV)\}$, as a function of the lattice momentum squared for the $16^3 \times 32$ lattices with $am_u = 0.03$. The off-diagonal mixing between operators is highly suppressed.

rotating back to the chirality basis, is shown in Fig. 3. We see that as expected, the off diagonal elements are negligible.

We now perform a mild chiral extrapolation and match to the $\overline{\mathrm{MS}}$ scheme at $\mu = 2$ GeV. This gives

$$U^{\overline{\mathrm{MS}}\leftarrow \mathrm{latt}}(2GeV)_{LL} = 0.662(10) \tag{4.7}$$
$$U^{\overline{\mathrm{MS}}\leftarrow \mathrm{latt}}(2GeV)_{RL} = 0.664(8) \tag{4.8}$$

## 5. Conclusion

The errors quoted so far have been purely statistical, we also have systematic errors to consider due to finite volume effects, extrapolating to the chiral limit, keeping the strange quark mass fixed and a systematic error due to our treatment of the NPR.

From Table 1 we can see that the values for the LECs on the two different volumes, agree within errors, from this we conclude there are no significant finite volume effects. For the fixed strange quark mass, we compare our result to the $N_f = 2$ result from [17] we see there is very good agreement. To estimate the error in taking a linear extrapolation to the chiral limit, we performed an extrapolation both with and without the lightest mass point. This gave results differing by 18% and 17% for $\alpha$ and $\beta$ respectively. For the NPR, we estimate a systematic error of 8%, which is dominated by the error in truncating the perturbative expansion for the matching factor at order $\alpha_s^2$.

Adding all of these uncertainties in quadrature, we estimate the low–energy parameters renormalised at $\mu = 2$ GeV to be:

$$\alpha = -0.0112 \pm 0.0012_{(\mathrm{stat})} \pm 0.0022_{(\mathrm{syst})}\ \mathrm{GeV}^3 \tag{5.1}$$
$$\beta = 0.0120 \pm 0.0013_{(\mathrm{stat})} \pm 0.0023_{(\mathrm{syst})}\ \mathrm{GeV}^3. \tag{5.2}$$

## References

[1] H. Murayama and A. Pierce, Phys. Rev. D **65** (2002) 055009 [arXiv:hep-ph/0108104].

[2] Poster presented by H. Nishino [Super-Kamiokande Collaboration] at Neutrino 08 (2008)

[3] B. L. Ioffe, Nucl. Phys. B **188** (1981) 317 [Erratum-ibid. B **191** (1981) 591].

[4] Y. Tomozawa, Phys. Rev. Lett. **46** (1981) 463 [Erratum-ibid. **49** (1982) 507].

[5] J. F. Donoghue and E. Golowich, Phys. Rev. D **26** (1982) 3092.

[6] S. Meljanac, D. Palle, I. Picek and D. Tadic, Nucl. Phys. B **206**, 298 (1982).

[7] N. V. Krasnikov, A. A. Pivovarov and N. N. Tavkhelidze, JETP Lett. **36** (1982) 333 [Pisma Zh. Eksp. Teor. Fiz. **36** (1982) 272].

[8] A. W. Thomas and B. H. J. Mckellar, Nucl. Phys. B **227**, 206 (1983).

[9] B. L. Ioffe and A. V. Smilga, Nucl. Phys. B **232**, 109 (1984).

[10] S. J. Brodsky, J. R. Ellis, J. S. Hagelin and C. T. Sachrajda, Nucl. Phys. B **238**, 561 (1984).

[11] Y. Hara, S. Itoh, Y. Iwasaki and T. Yoshie, Phys. Rev. D **34**, 3399 (1986).

[12] K. C. Bowler, D. Daniel, T. D. Kieu, D. G. Richards and C. J. Scott, Nucl. Phys. B **296**, 431 (1988).

[13] M. B. Gavela, S. F. King, C. T. Sachrajda, G. Martinelli, M. L. Paciello and B. Taglienti, Nucl. Phys. B **312**, 269 (1989).

[14] S. Aoki *et al.* [JLQCD Collaboration], Phys. Rev. D **62**, 014506 (2000) [arXiv:hep-lat/9911026].

[15] N. Tsutsui *et al.* [CP-PACS Collaboration and JLQCD Collaborations], Phys. Rev. D **70**, 111501 (2004) [arXiv:hep-lat/0402026].

[16] Y. Aoki *et al.* [RBC-UKQCD Collaboration], arXiv:0806.1031 [hep-lat].

[17] Y. Aoki, C. Dawson, J. Noaki and A. Soni, Phys. Rev. D **75**, 014507 (2007) [arXiv:hep-lat/0607002].

[18] S. Weinberg, Phys. Rev. Lett. **43**, 1566 (1979).

[19] F. Wilczek and A. Zee, Phys. Rev. Lett. **43**, 1571 (1979).

[20] L. F. Abbott and M. B. Wise, Phys. Rev. D **22**, 2208 (1980).

[21] M. Claudson, M. B. Wise and L. J. Hall, Nucl. Phys. B **195**, 297 (1982).

[22] C. Amsler *et al.* [Particle Data Group], Phys. Lett. B **667**, 1 (2008).

[23] S. Y. Hsueh *et al.*, Phys. Rev. D **38**, 2056 (1988).

[24] J. Hisano, H. Murayama and T. Yanagida, Nucl. Phys. B **402** (1993) 46 [arXiv:hep-ph/9207279].

[25] C. Allton *et al.* [RBC and UKQCD Collaborations], Phys. Rev. D **76**, 014504 (2007) [arXiv:hep-lat/0701013].

[26] C. Allton *et al.*, arXiv:0804.0473 [hep-lat].

[27] D. J. Antonio *et al.* [RBC and UKQCD Collaborations], Phys. Rev. D **75**, 114501 (2007) [arXiv:hep-lat/0612005].

[28] D. Toussaint and W. Freeman, arXiv:0808.2211 [hep-lat].